A Block Solver for the Exponentially Fitted IIPG-0 Method

AQ1 Blanca Ayuso de Dios[1], Ariel Lombardi[2], Paola Pietra[3], and Ludmil Zikatanov[4]

[1] Centre de Recerca Matemàtica, Barcelona, Spain. bayuso@crm.cat
[2] Departamento de Matemática, Universidad de Buenos Aires & CONICET, Argentina. aldoc7@dm.uba.ar
[3] IMATI-CNR, Pavia , Italy , pietra@imati.cnr.it
[4] Department of Mathematics, Penn State University, USA ltz@math.psu.edu

Summary. We consider an exponentially fitted discontinuous Galerkin method for advection dominated problems and propose a block solver for the resulting linear systems. In the case of strong advection the solver is robust with respect to the advection direction and the number of unknowns.

1 Introduction

Let $\Omega \subset \mathbb{R}^2$ be a polygon, $f \in L^2(\Omega), g \in H^{1/2}(\partial\Omega)$ and let $\varepsilon > 0$ be constant. We consider the advection-diffusion problem

$$-\operatorname{div}(\varepsilon\nabla u - \beta u) = f \quad \text{in } \Omega, \qquad u = g \quad \text{on } \partial\Omega, \tag{1}$$

where $\beta \in [W^{1,\infty}(\Omega)]^2$ derives from a potential $\beta = \nabla\psi$. In applications to semiconductor devices, u is the electron density, ψ the electrostatic potential and the electric field $|\nabla\psi|$ might be fairly large in some parts of Ω, so that (1) becomes advection dominated. Its robust numerical approximation and the design of efficient solvers, are still a challenge. Exponential fitting [2] and discontinuous Galerkin (DG) are two approaches that have been combined in [3] to develop exponentially fitted DG methods (in primal and mixed formulation). In this note, we consider a variant of these schemes, based on the use of the Incomplete Interior Penalty IIPG-0 method and propose an efficient solver for the resulting linear systems.

The change of variable $\rho := e^{-\frac{\psi}{\varepsilon}}u$ in the problem (1) leads to

$$-\nabla\cdot(\kappa\nabla\rho) = f \text{ in } \Omega, \quad \rho = \chi \text{ on } \partial\Omega\ , \tag{2}$$

where $\kappa := \varepsilon e^{\frac{\psi}{\varepsilon}}$ and $\chi := e^{-\frac{\psi}{\varepsilon}}g$. An IIPG-0 approximation to (2) gives rise to the EF-IIPG-0 scheme for (1). We propose a block solver that uses ideas from [1] and reduce the solution to that of an exponentially fitted Crouziex-Raviart (CR) discretization,

R. Bank et al. (eds.), *Domain Decomposition Methods in Science and Engineering XX*, Lecture Notes in Computational Science and Engineering 91,
DOI 10.1007/978-3-642-35275-1__27, © Springer-Verlag Berlin Heidelberg 2013

which has much less degrees of freedom. The associated (CR) matrix is further reduced to an approximate block lower triangular form, which is efficiently solved by a block Gauss-Siedel algorithm.

In our description we focus on the case $\beta = \nabla\psi$ piecewise constant; although we include some numerical results for a more general case (cf. Test 2). Extensions of the method (allowing ψ to be discontinuous) and further analysis of the proposed solvers are topics of current research.

2 The Exponentially Fitted IIPG-0 Method

Let $\mathscr{T}_h$ be a shape-regular family of partitions of Ω into triangles T and let $h = \max_{T\in\mathscr{T}_h} h_T$ with h_T denoting the diameter of T for each $T \in \mathscr{T}_h$. We assume $\mathscr{T}_h$ does not contain hanging nodes. We denote by $\mathscr{E}_h^o$ and $\mathscr{E}_h^\partial$ the sets of all interior and boundary edges, respectively, and we set $\mathscr{E}_h = \mathscr{E}_h^o \cup \mathscr{E}_h^\partial$.

Let T^+ and T^- be two neighboring elements, and $\mathbf{n}^+$, $\mathbf{n}^-$ be their outward normal unit vectors, respectively ($\mathbf{n}^\pm = \mathbf{n}_{T^\pm}$). Let $\zeta^\pm$ and $\boldsymbol{\tau}^\pm$ be the restriction of ζ and $\boldsymbol{\tau}$ to $T^\pm$. We define the average and jump trace operators:

$$\begin{aligned} 2\{\zeta\} &= (\zeta^+ + \zeta^-), \quad [\![\zeta]\!] = \zeta^+\mathbf{n}^+ + \zeta^-\mathbf{n}^- && \text{on } E \in \mathscr{E}_h^o, \\ 2\{\boldsymbol{\tau}\} &= (\boldsymbol{\tau}^+ + \boldsymbol{\tau}^-), \quad [\![\boldsymbol{\tau}]\!] = \boldsymbol{\tau}^+\cdot\mathbf{n}^+ + \boldsymbol{\tau}^-\cdot\mathbf{n}^- && \text{on } E \in \mathscr{E}_h^o, \end{aligned}$$

and on $e \in \mathscr{E}_h^\partial$ we set $[\![\zeta]\!] = \zeta\mathbf{n}$ and $\{\boldsymbol{\tau}\} = \boldsymbol{\tau}$. We will also use the notation

$$(u,w)_{\mathscr{T}_h} = \sum_{T\in\mathscr{T}_h}\int_T uw dx \qquad \langle u,w\rangle_{\mathscr{E}_h} = \sum_{e\in\mathscr{E}_h}\int_e uw ds \quad \forall u,w, \in V^{DG},$$

where V^{DG} is the discontinuous linear finite element space defined by:

$$V^{DG} = \left\{u \in L^2(\Omega) \,:\, u_{|_T} \in \mathbb{P}^1(T)\ \forall T \in \mathscr{T}_h\right\},$$

Here, $\mathbb{P}^1(T)$ is the space of linear polynomials on T. Similarly, $\mathbb{P}^0(T)$ and $\mathbb{P}^0(e)$ are the spaces of constant polynomials on T and e, respectively. For each $e \in \mathscr{E}_h$, let $\mathscr{P}_e^0 : L^2(e) \mapsto \mathbb{P}^0(e)$ (resp. $\mathscr{P}_T^0 : L^2(T) \mapsto \mathbb{P}^0(T)$, for each $T \in \mathscr{T}_h$) be the L^2-orthogonal projections defined by

$$\mathscr{P}_e^0(u) := \frac{1}{|e|}\int_e u, \quad \forall u \in L^2(e), \quad \mathscr{P}_T^0(v) := \frac{1}{|T|}\int_T v, \quad \forall v \in L^2(T).$$

We denote by V^{CR} the classical Crouziex-Raviart (CR) space:

$$V^{CR} = \left\{v \in L^2(\Omega) \,:\, v_{|_T} \in \mathbb{P}^1(T) \forall T \in \mathscr{T}_h \text{ and } \mathscr{P}_e^0[\![v]\!] = 0\ \forall e \in \mathscr{E}_h\right\}.$$

Note that $v = 0$ at the midpoint m_e of each $e \in \mathscr{E}_h^\partial$. To represent the functions in V^{DG} we use the basis $\{\varphi_{e,T}\}_{T\in\mathscr{T}_h, e\in\mathscr{E}_h}$, defined by

$$\forall T \in \mathscr{T}_h \quad \varphi_{e,T}(x) \in \mathbb{P}^1(T) \quad e \subset \partial T \quad \varphi_{e,T}(m_{e'}) = \delta_{e,e'} \quad \forall e' \in \mathscr{E}_h\,. \tag{3}$$

In particular, any $w \in \mathbb{P}^1(T)$ can be written as $w = \sum_{e \subset \partial T} w(m_e)\varphi_{e,T}$.

We first consider the IIPG-0 approximation to the solution of (2): Find $\rho \in V^{DG}$ such that $\mathscr{A}(\rho, w) = (f, w)_{\mathscr{T}_h}$ for all $w \in V^{DG}$ with

$$\mathscr{A}(\rho,w) = (\kappa_T^* \nabla \rho, \nabla w)_{\mathscr{T}_h} - \langle \{\kappa_T^* \nabla \rho\}, [\![w]\!] \rangle_{\mathscr{E}_h} + \langle S_e \{[\![\rho]\!]\}, \mathscr{P}^0([\![w]\!]) \rangle_{\mathscr{E}_h}\,. \tag{4}$$

Here, S_e is the penalty parameter and $\kappa_T^* \in \mathbb{P}^0(T)$ the harmonic average approximation to $\kappa = \varepsilon e^{\psi/\varepsilon}$ both defined in [3] by:

$$\kappa_T^* := \frac{1}{\mathscr{P}_T^0(\kappa^{-1})} = \frac{\varepsilon}{\mathscr{P}_T^0(e^{-\frac{\psi}{\varepsilon}})}\,, \qquad S_e := \alpha_e h_e^{-1}\{\kappa_T^*\}_e\,, \tag{5}$$

Next, following [3] we introduce the local operator $\mathfrak{T} : V^{DG} \mapsto V^{DG}$ that approximates the change of variable introduced before (2):

$$\mathfrak{T}w := \sum_{T \in \mathscr{T}_h} (\mathfrak{T}w)|_T = \sum_{T \in \mathscr{T}_h} \sum_{e \subset \partial T} \mathscr{P}_e^0(e^{-\frac{\psi}{\varepsilon}}) w(m_e) \varphi_{e,T} \quad \forall w \in V^{DG}\,. \tag{6}$$

By setting $\rho := \mathfrak{T}u$ in (4), we finally get the EF-IIPG-0 approximation to (1):

Find $u_h \in V^{DG}$ s.t. $\mathscr{B}(u_h, w) := \mathscr{A}(\mathfrak{T}u_h, w) = (f, w)_{\mathscr{T}_h}$ $\forall w \in V^{DG}$ with

$$\mathscr{B}(u,w) = (\kappa_T^* \nabla \mathfrak{T}u, \nabla w)_{\mathscr{T}_h} - \langle \{\kappa_T^* \nabla \mathfrak{T}u\}, [\![w]\!] \rangle_{\mathscr{E}_h} + \langle S_e \{[\![\mathfrak{T}u]\!]\}, \mathscr{P}^0[\![w]\!] \rangle_{\mathscr{E}_h}\,. \tag{7}$$

It is important to emphasize that the use of harmonic average to approximate $\kappa = \varepsilon e^{\psi/\varepsilon}$ as defined in (5) together with the definition of the local approximation of the change of variables prevents possible overflows in the computations when $|\nabla\psi|$ is large and ε is small. (See [3] for further discussion).

Also, these two ingredients are essential to ensure that the resulting method has an automatic upwind mechanism built-in that allows for an accurate approximation of the solution of (1) in the advection dominated regime. We will discuss this in more detail in Sect. 3.

Prior to close this section, we define for each $e \in \mathscr{E}_h$ and $T \in \mathscr{T}_h$:

$$\psi_{m,e} := \min_{x \in e} \psi(x) \quad \psi_{m,T} := \min_{x \in T} \psi(x); \quad \psi_{m,T} \leq \psi_{m,e} \text{ for } e \subset \partial T\,.$$

In the advection dominated regime $\varepsilon \ll |\beta| h = |\nabla\psi| h$

$$\mathscr{P}_T^0(e^{-(\psi/\varepsilon)}) \simeq \varepsilon^2 e^{-\frac{\psi_{m,T}}{\varepsilon}} \qquad \mathscr{P}_{e_i}^0(e^{-\psi/\varepsilon}) \simeq \varepsilon\, e^{-\frac{\psi_{m,e}}{\varepsilon}}\,. \tag{8}$$

The first of the above scalings together with the definitions in (5) implies

$$\kappa_T^* \simeq \frac{1}{\varepsilon} e^{\frac{\psi_{m,T}}{\varepsilon}}\,, \qquad S_e \simeq \frac{\alpha}{2\varepsilon} |e|^{-1} e^{\frac{(\psi_{m,T_1} + \psi_{m,T_2})}{\varepsilon}} \quad e = \partial T_1 \cap \partial T_2\,. \tag{9}$$

3 Algebraic System and Properties

Let A and B be the operators associated to the bilinear forms $\mathscr{A}(\cdot,\cdot)$ (4) and $\mathscr{B}(\cdot,\cdot)$ (7), respectively. We denote by $\mathbb{A}$ and $\mathbb{B}$ their matrix representation in the basis $\{\varphi_{e,T}\}_{T\in\mathscr{T}_h, e\in\mathscr{E}_h}$ (3). In this basis, the operator $\mathfrak{T}$ defined in (6) is represented as a diagonal matrix, $\mathbb{D}$, and $\mathbb{B}=\mathbb{A}\mathbb{D}$. Thus, the approximation to (2) and (1) amounts to solve the linear systems (of dimension $2n_e - n_b$; with n_e and n_b being the cardinality of $\mathscr{E}_h$ and $\mathscr{E}_h^{\partial}$, respectively):

$$\mathbb{A}\boldsymbol{\rho} = \boldsymbol{F}\,, \quad \text{and} \quad \mathbb{D}\boldsymbol{u} = \boldsymbol{\rho} \qquad \text{or} \qquad \mathbb{B}\boldsymbol{u} = \widetilde{\boldsymbol{F}}\,, \tag{10}$$

where $\boldsymbol{\rho},\boldsymbol{u},\boldsymbol{F}$ and $\widetilde{\boldsymbol{F}}$ are the vector representations of ρ, u and the right hand sides of the approximate problems. From the definition (6) of $\mathfrak{T}$ it is easy to deduce the scaling of the entries of the diagonal matrix $\mathbb{D}=(d_{i,i})_{i=1}^{2n_e-n_b}$.

$$\mathbb{D}=(d_{i,j})_{i,j=1}^{2n_e-n_b} \quad d_{i,i}=\mathscr{P}^0_{e_i}(e^{-\psi/\varepsilon}) \simeq \varepsilon e^{-\frac{\psi_{m,e}}{\varepsilon}}, \quad d_{i,j}\equiv 0 \quad i\neq j\,.$$

We now revise a result from [1]:

Proposition 1. *Let $\mathscr{Z}\subset V^{DG}$ be the space defined by*

$$\mathscr{Z}=\left\{z\in L^2(\Omega) : z_{|_T} \in \mathbb{P}^1(T)\,\forall T\in\mathscr{T}_h \text{ and } \mathscr{P}^0_e\{v\}=0\,\forall e\in\mathscr{E}_h^o\right\}.$$

Then, for any $w\in V^{DG}$ there exists a unique $w^{cr}\in V^{CR}$ and a unique $w^z\in\mathscr{Z}$ such that $w=w^{cr}+w^z$, that is: $V^{DG}=V^{CR}\oplus\mathscr{Z}$. Moreover, $\mathscr{A}(w^{cr},w^z)=0\,\forall w^{cr}\in V^{CR}$, and $\forall w^z\in\mathscr{Z}$.

Proposition 1 provides a simple *change of basis* from $\{\varphi_{e,T}\}$ to canonical basis in V^{CR} and $\mathscr{Z}$ that results in the following algebraic structure for (10):

$$\boldsymbol{\rho}=\begin{bmatrix}\boldsymbol{\rho}^z\\ \boldsymbol{\rho}^{cr}\end{bmatrix}, \qquad \mathbb{A}=\begin{bmatrix}\mathbb{A}^{zz} & \mathbf{0}\\ \mathbb{A}^{vz} & \mathbb{A}^{vv}\end{bmatrix}, \qquad \mathbb{B}=\begin{bmatrix}\mathbb{B}^{zz} & 0\\ \mathbb{B}^{vz} & \mathbb{B}^{vv}\end{bmatrix}. \tag{11}$$

Due to the assumed continuity of ψ, $\mathbb{D}$ is still diagonal in this basis. The algebraic structure (11) suggests the following exact solver:

The solution $u=u^z+u^{cr}$ satisfying $\mathscr{B}(u,w)=(f,w)_{\mathscr{T}_h}$, for all $w\in V^{DG}$ is then obtained by

1. Solve for u^z: $\mathscr{B}(u^z,w^z)=(f,w^z)_{\mathscr{T}_h} \quad \forall w^z\in\mathscr{Z}$.
2. Solve for u^{cr}: $\mathscr{B}(u^{cr},w^{cr})=(f,w^{cr})_{\mathscr{T}_h}-\mathscr{B}(u^z,w^{cr}) \quad \forall w^{cr}\in V^{CR}$.

Next, wet discuss how to solve efficiently each of the above steps.

Step 1: Solution in the $\mathscr{Z}$-space. In [1] it was shown that A^{zz} is a diagonal positive definite matrix. This is also true for $\mathbb{B}^{zz}$ since it is the product of two diagonal matrices. The continuity of ψ implies

$$\mathscr{B}(u^z, w^z) = \langle S_e \mathfrak{T}[\![u^z]\!], \mathscr{P}_e^0([\![w^z]\!])\rangle_{\mathscr{E}_h} \quad \forall\, u^z, w^z \in \mathscr{Z}\,. \tag{12}$$

Using (8) and (5) we observe that the entries of $\mathbb{B}^{zz}$ scale as:

$$\mathbb{B}^{zz} = (b_{i,j})_{i=1}^{n_e} \qquad b_{i,j} = S_{e_i}|e_i|d_j\delta_{i,j} \simeq \delta_{i,j}\frac{\alpha}{2}\, e^{-(\psi_{m,e}-\psi_{m,T_1}-\psi_{m,T_2})/\varepsilon}$$

which are always positive, so in particular $\mathbb{B}^{zz}$ it is also an M-matrix.

Step 2: Solution in V^{CR}. In [1] it was shown that the block $\mathbb{A}^{vv}$ coincides with the stiffness matrix of a CR discretization of (2), and so it is an s.p.d. matrix. However, this is no longer true for $\mathbb{B}^{vv}$ which is positive definite but non-symmetric.

$$\mathscr{B}(u^{cr}, w^{cr}) = (\kappa_T^* \nabla \mathfrak{T} u^{cr}, \nabla w^{cr})_{\mathscr{T}_h} \quad \forall\, u^{cr}, w^{cr} \in V^{CR}\,.$$

In principle, the sparsity pattern of $\mathbb{B}^{vv}$ is that of a symmetric matrix. Using (8) and (5), we find that the entries of the matrix scale as:

$$\mathbb{B}^{vv} = \left(b_{i,j}^{cr}\right)_{i,j}^{n_{cr}:=n_e-n_b} \qquad b_{i,j}^{cr} := \kappa_T^* \frac{|e_i||e_j|}{|T|}\mathbf{n}_{e_i}\cdot \mathbf{n}_{e_j} d_j \simeq e^{-\frac{(\psi_{m,e}-\psi_{m,T})}{\varepsilon}} \tag{13}$$

Since ψ is assumed to be piecewise linear, for each T, it attains its minimum (and also its maximum) at a vertex of T, say $\boldsymbol{x_0}$ and $\psi_{m,e}$ is attained at one of the vertex of the edge e, say $\boldsymbol{x_e}$. In particular, this implies that

$$\psi_{m,e} - \psi_{m,T} \approx \nabla\psi \cdot (\boldsymbol{x_e} - \boldsymbol{x_0}) = \beta \cdot (\boldsymbol{x_e} - \boldsymbol{x_0}) = \begin{cases} 0 & \boldsymbol{x_e} = \boldsymbol{x_0} \\ |\beta| h & \boldsymbol{x_e} \neq \boldsymbol{x_0} \end{cases}$$

Hence, in the advection dominated case $\varepsilon \ll |\beta| h$ some of the entries in (13) vanish (up to machine precision) for ε small; this is the automatic upwind mechanism intrinsic of the method. As a consequence, the sparsity pattern of $\mathbb{B}^{vv}$ is no longer symmetric and this can be exploited to re-order the unknowns so that $\mathbb{B}^{vv}$ can be reduced to block lower triangular form.

Notice also that for $\mathscr{T}_h$ acute, the block $\mathbb{A}^{vv}$ being the stiffness matrix of the Crouziex-Raviart approximation to (2), is an M-matrix. Hence, since the block $\mathbb{B}^{vv}$ is the product of a positive diagonal matrix and $\mathbb{A}^{vv}$, it will also be an M-matrix if the triangulation is acute (see [2]).

4 Block Gauss-Siedel Solver for V^{CR}-Block

We now consider re-orderings of the unknowns (dofs), which reduce $\mathbb{B}^{vv}$ to block lower triangular form. For such reduction, we use the algorithm from [4] which roughly amounts to *partitioning* the set of dofs into non-overlapping blocks. In the strongly advection dominated case the size of the resulting blocks is small and a block Gauss-Seidel method is an efficient solver. Such techniques have been studied in [5] for conforming methods.

The idea is to consider the *directed* graph $\boldsymbol{G} = (\boldsymbol{V}, \boldsymbol{E})$ associated with $\mathbb{B}^{vv} \in \mathbb{R}^{n_{cr} \times n_{cr}}$; $\boldsymbol{G}$ has n_{cr} vertices labeled $\boldsymbol{V} = \{1, \dots, n_{cr}\}$ and its set of *edges* $\boldsymbol{E}$ has cardinality equal to the number of nonzero entries[5] of $\mathbb{B}^{vv}$. By definition, $(i,j) \in \boldsymbol{E}$ *iff* $b^{cr}_{ij} \neq 0$. Note that in the advection dominated case, the built-in upwind mechanism results in a non-symmetric sparsity pattern for $\mathbb{B}^{vv}$ (see the last two paragraphs of Sect. 3). Thus, we may have $(i,j) \in \boldsymbol{E}$, while $(j,i) \notin \boldsymbol{E}$. Then, the problem of reducing $\mathbb{B}^{vv}$ to block lower triangular form of $\mathbb{B}^{vv}$ is equivalent to partitioning $\boldsymbol{G}$ as a union of strongly connected components.
Such partitioning induces non-overlapping partitioning of the set of dofs, $\boldsymbol{V} = \cup_{i=1}^{N_b} \omega_i$. For $i = 1, \dots, N_b$, let m_i denote the cardinality of ω_i; let $\mathbb{I}_i \in \mathbb{R}^{n_{cr} \times m_i}$ be the matrix that is identity on dofs in ω_i and zero otherwise; and $\mathbb{B}^{vv}_i = \mathbb{I}^T_i \mathbb{B}^{vv} \mathbb{I}_i$ is the block corresponding to the dofs in ω_i. The block Gauss–Seidel algorithm reads: *Let* $\boldsymbol{u}^{cr}_0$ *be given, and assume* $\boldsymbol{u}^{cr}_k$ *has been obtained. Then* $\boldsymbol{u}^{cr}_{k+1}$ *is computed via:* For $i = 1, \dots N_b$

$$\boldsymbol{u}^{cr}_{k+i/N_b} = \boldsymbol{u}^{cr}_{k+(i-1)/N_b} + \mathbb{I}_i (\mathbb{B}^{vv}_i)^{-1} \mathbb{I}^T_i \left(\boldsymbol{F} - \mathbb{B}^{vv} \boldsymbol{u}^{cr}_{k+(i-1)/N_b} \right). \tag{14}$$

As we report in Sect. 5, the action of $(\mathbb{B}^{vv}_i)^{-1}$ can be computed exactly since in the advection dominated regime the size of the blocks $\mathbb{B}^{vv}_i$ is small.

5 Numerical Results

We present a set of numerical experiments to assess the performance of the proposed block solver. The tests refer to problem (2) with $\varepsilon = 10^{-3}, 10^{-5}, 10^{-7}$, and Ω is triangulated with a family of unstructured triangulations $\mathscr{T}_h$. In the tables given below $J = 1$ corresponds to the coarsest grid and each refined triangulation on level J, $J = 2, 3, 4$ is obtained by subdividing each of the $T \in \mathscr{T}_h$ on level $(J-1)$ into four congruent triangles. From the number of triangles n_T the total number of dofs for the DG approximation is $3n_T$.

Test 1. Boundary Layer: $\Omega = (-1,1)^2$, $\beta = [1,1]^t$, $n_T = 112$ for the coarsest mesh and f is such that the exact solution is given by

$$u(x,y) = \left(x + \frac{1 + e^{-2/\varepsilon} - 2e^{(x-1)/\varepsilon}}{1 - e^{-2/\varepsilon}} \right) \left(y + \frac{1 + e^{-2/\varepsilon} - 2e^{(y-1)/\varepsilon}}{1 - e^{-2/\varepsilon}} \right).$$

Test 2. Rotating Flow: $\Omega = (-1,1)^{\times}(0,1)$, $f = 0$ and $\mathrm{curl}\beta \neq 0$,

[5] Each dof corresponds to a vertex in the graph; each nonzero entry to an edge.

$$\beta = \begin{bmatrix} 2y(1-x^2) \\ -2x(1-y^2) \end{bmatrix}^t \qquad g(x,y) = \begin{cases} 1+\tanh(10(2x+1)) & x \le 0,\ y=0, \\ 0 & \text{elsewhere}\,. \end{cases}$$

We stress that this test does not fit in the simple description given here, and special care is required (see [3]). For the approximation, for each $T \in \mathscr{T}_h$, with barycenter (x_T, y_T), we use the approximation

$$\beta|_T \approx \nabla\psi|_T \qquad \text{with} \qquad \psi|_T = 2y_T(1-x_T^2)x - 2x_T(1-2y_T^2)y\,,$$

and so ψ is discontinuous. The coarsest grid has $n_T = 224$ triangles. In Fig. 1 are

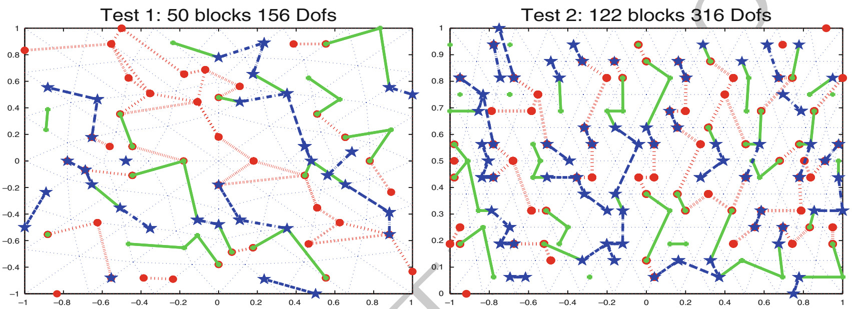

Fig. 1. Plot of the connected components (*blocks*) of $\mathbb{B}^{vv}$ created during Tarjan's algorithm: Test 1 with $\varepsilon = 10^{-5}$ (*left*); Test 2 with $\varepsilon = 10^{-7}$ (*right*)

represented the plot of the strongly connected components of the graph depicting the blocks for $\mathbb{B}^{vv}$ created during Tarjan's algorithm, on the coarsest meshes; for Test 1 with $\varepsilon = 10^{-5}$ (left figure) and for Test 2 with $\varepsilon = 10^{-7}$ (right figure). We have used different line types (and colors) to distinguish strongly connected components in the directed graph. In Table 1 we report the number of blocks N_b created during Tarjan's algorithm; the maximum size of the largest such block (M_b); the average block size (n_{av}); and the number of block-Gauss-Seidel iterations. After Tarjan's algorithm is used to re-order the matrix $\mathbb{B}^{vv}$, we use the block Gauss-Seidel algorithm (14) where each small block is solved exactly. In the tests that we report here and also in all other similar tests that we have done (with similar advection dominance) the number of block-Gauss-Seidel iterations and the size of the blocks is uniformly bounded with respect to the number of dofs when the advection strongly dominates. Thus, the computational cost for one block Gauss-Seidel iteration in the advection dominated regime is the same as the cost of performing a fixed number of matrix vector multiplications and the algorithm is optimal in such regime.

Acknowledgments This work started while the first two authors were visiting the IMATI-CNR, Pavia in October 2010. Thanks go to the IMATI for the hospitality and support. First author was partially supported by MEC grants MTM2008-03541 and MTM2011-27739-C04-04. Second author was supported by CONICET, Argentina. Last author was supported in part by National Science Foundation NSF-DMS 0810982.

		Test 1					Test 2			
ε \ J		1	2	3	4	ε \ J	1	2	3	4
10^{-3}	N_b	44	150	484	1182	N_b	31	1	1	1
	M_b	23	47	95	191	M_b	211	1304	5296	21344
	n_{av}	3.55	4.32	5.45	9.02	n_{av}	10.19	1304	5296	21344
	iters	7	19	43	166	iters	10	1	1	1
10^{-5}	N_b	50	210	866	3474	N_b	122	468	1822	7106
	M_b	23	47	95	191	M_b	4	4	7	37
	n_{av}	3.12	3.08	3.05	3.07	n_{av}	2.59	2.78	2.91	3.00
	iters	4	4	4	14	iters	4	4	7	24
10^{-7}	N_b	50	210	866	3522	N_b	122	468	1832	7247
	M_b	23	47	95	191	M_b	4	4	4	6
	n_{av}	3.12	3.08	3.05	3.03	n_{av}	2.59	2.78	2.89	2.95
	iters	4	4	4	4	iters	4	4	4	4

Table 1. Number of blocks (N_b) created during the Tarjan's ordering algorithm, size of largest block (M_b), average size of blocks (n_{av}) and number of block-Gauss-Seidel iterations (iters) for Test 1 (left) and Test 2 (right).

Bibliography

[1] Blanca Ayuso de Dios and Ludmil Zikatanov. Uniformly convergent iterative methods for discontinuous Galerkin discretizations. *J. Sci. Comput.*, 40(1–3): 4–36, 2009.

[2] F. Brezzi, L. D. Marini, S. Micheletti, P. Pietra, R. Sacco, and S. Wang. Discretization of semiconductor device problems. I. In *Handbook of numerical analysis. Vol. XIII*, pages 317–441. North-Holland, Amsterdam, 2005.

[3] Ariel Lombardi and P. Pietra. Exponentially fitted discontinuous galerkin schemes for singularly perturbed problems. numerical methods for partial differential equations. 2011. (to appear) doi: 10.1002/num.20701.

[4] Robert Tarjan. Depth-first search and linear graph algorithms. *SIAM J. Comput.*, 1(2):146–160, 1972.

[5] Feng Wang and Jinchao Xu. A crosswind block iterative method for convection-dominated problems. *SIAM J. Sci. Comput.*, 21(2):620–645, 1999.